

**Measurement of  $B(M1)$  for the  $\pi p_{3/2} \nu p_{1/2}^{-1}$  doublet in  $^{68}\text{Cu}$** 

L. Hou,\* T. Ishii,† and M. Asai

*Advanced Science Research Center, Japan Atomic Energy Research Institute, Tokai, Ibaraki 319-1195, Japan*

J. Hori‡

*Department of Fusion Engineering Research, Japan Atomic Energy Research Institute, Tokai, Ibaraki 319-1195, Japan*

K. Ogawa and H. Nakada

*Department of Physics, Faculty of Science, Chiba University, Inage, Chiba 263-8522, Japan*

(Received 12 May 2003; published 18 November 2003; publisher error corrected 26 November 2003)

Lifetimes of excited states in  $^{68}\text{Cu}$  were measured by the  $\gamma$ - $\gamma$ - $t$  coincidence using two  $\text{BaF}_2$  detectors through the decay of  $^{68}\text{Cu}^m$  produced by the  $(n, p)$  reaction. The half-life of the  $2^+$  state at 84 keV was obtained as 7.84(8) ns, corresponding to the  $B(M1; 2^+ \rightarrow 1^+)$  value of  $0.00777(8)\mu_N^2$ . A shell model calculation with a minimum model space of  $\pi p_{3/2} \nu p_{1/2}^{-1}$  gives a good prediction of this  $B(M1)$  value by using experimental  $g$  factors of neighboring nuclei. This small  $B(M1)$  value can also be explained by a shell model calculation in the  $f_{7/2}^r(p_{3/2}f_{5/2}p_{1/2})^{n+r}$  ( $r=0, 1$ ) model space.

DOI: 10.1103/PhysRevC.68.054306

PACS number(s): 21.10.Tg, 23.20.-g, 21.60.Cs, 27.50.+e

**I. INTRODUCTION**

The nuclear structure around  $^{68}\text{Ni}$ , with  $Z=28$  and  $N=40$ , provides important knowledge of the shell structure in the neutron-rich Ni region and thus many studies have been made with the progress of experimental techniques [1–18]. Among these studies, the magic properties of  $^{68}\text{Ni}$  have been discussed from different angles. One of the issues is whether one can treat the  $^{68}\text{Ni}$  nucleus as a core in a shell model calculation. We previously demonstrated that the energy levels in  $^{71}\text{Cu}$  can be predicted very accurately by a shell model calculation with the  $\pi p_{3/2} \nu g_{9/2}^2$  model space, using experimental energy levels in neighboring nuclei as residual two-body interactions [7]. It is interesting to study to what extent such a calculation is valid to explain the properties of nuclei around  $^{68}\text{Ni}$ .

In the  $^{68}\text{Cu}_{39}$  nucleus, the proton ( $\pi$ )  $p_{3/2}$  and the neutron ( $\nu$ )  $p_{1/2}$  orbitals lie near the Fermi surface. Therefore, the  $1^+$  ground state and the  $2^+$  first excited state in  $^{68}\text{Cu}$  are expected to have a large component of the  $\pi p_{3/2} \nu p_{1/2}^{-1}$  configuration. This simple configuration gives an insight into the nuclear structure around  $^{68}\text{Ni}$ . In particular, the  $B(M1; 2^+ \rightarrow 1^+)$  value provides a good test of a shell model calculation. Furthermore, this  $B(M1)$  value gives information on the core excitation, in particular, for the  $Z, N=28$  core.

Excited states in  $^{68}\text{Cu}$  were first studied through the  $\gamma$  decay of the  $^{68}\text{Cu}$  isomer ( $T_{1/2}=3.75$  min) produced by the  $^{68}\text{Zn}(n, p)$  reaction [19–22]. Sherman *et al.* [23] studied energy levels in  $^{68}\text{Cu}$  by the  $(t, ^3\text{He})$  transfer reaction. Recently, the  $g$  factors of the ground and the isomeric states were mea-

sured in  $^{68}\text{Cu}$  separated from fission products using a mass separator with a chemically selective laser-ion-source [24]. We found a nanosecond isomer in  $^{68}\text{Cu}$  [25] produced in heavy-ion deep-inelastic collisions using an isomer-scope [26].

In the present study, we have carried out a decay experiment of  $^{68}\text{Cu}^m$  produced by the  $^{68}\text{Zn}(n, p)$  reaction using 14-MeV neutrons. This reaction provides an almost pure  $^{68}\text{Cu}^m$  source without chemical or mass separation. We have measured the lifetime of the first excited state and obtained a small  $B(M1; 2^+ \rightarrow 1^+)$  value. We show that a parameter-free shell model calculation within the  $\pi p_{3/2} \nu p_{1/2}^{-1}$  model space correctly predicts this  $B(M1)$  value by using experimental  $g$  factors of neighboring nuclei. Furthermore, we show that this small  $B(M1)$  value can be explained by a shell model calculation in the  $f_{7/2}^r(p_{3/2}f_{5/2}p_{1/2})^{n+r}$  ( $r=0, 1$ ) model space.

**II. EXPERIMENTS**

The  $^{68}\text{Cu}^m$  source ( $T_{1/2}=3.75$  min) was produced by the  $^{68}\text{Zn}(n, p)$  reaction at FNS (fusion neutronics source) in JAERI. Three  $^{68}\text{Zn}$  targets of 0.2 g and 10 mm in diameter were prepared from the 99.4% enriched  $^{68}\text{ZnO}$  powder by the following procedure. The  $^{68}\text{ZnO}$  powder was dissolved in a 0.1M  $\text{H}_2\text{SO}_4$  solution. Then, the  $^{68}\text{Zn}$  metal was deposited by electrolysis on a thin platinum wire. The  $^{68}\text{Zn}$  metal removed from the Pt wire was shaped by pressing it in a mold 10 mm in diameter. Each target was sealed in thin paraffin paper and in a polyethylene film.

The  $^{68}\text{Zn}$  target was irradiated by 14-MeV neutrons at a place of about  $5 \times 10^9 \text{ cm}^{-2} \text{ s}^{-1}$  neutron flux; FNS generates  $4 \times 10^{12} \text{ s}^{-1}$  neutrons by the  $^3\text{H}(d, n)$  reaction using a 37 TBq tritium rotating target. The  $^{68}\text{Zn}$  target was irradiated for 10 min and then transferred through a pneumatic tube to the outside of the irradiation room. The irradiated target was cooled for about 2 min. Thus, the cycle of 10-min irradiation, 2-min cooling, and 8-min measurement was repeated

\*On leave from China Institute of Atomic Energy, P.O. Box 275(67), Beijing 102413, China.

†Electronic address: ishii@popsvr.tokai.jaeri.go.jp

‡Present address: Kyoto University Research Reactor Institute, Kumatori, Osaka 590-0494, Japan.

using three  $^{68}\text{Zn}$  targets. Since the production cross section of  $^{68}\text{Cu}^m$  is 5 mb [27], the activity of the  $^{68}\text{Cu}^m$  source was about 30 kBq at the beginning of the measurement.

Lifetimes of excited states in  $^{68}\text{Cu}$  were measured using two  $\text{BaF}_2$  detectors of 25 mm in diameter and 10 mm in thickness. These detectors were placed face to face at a distance of 20 mm and the  $^{68}\text{Cu}^m$  source was placed at the center between them. A  $\beta$ -ray absorber made of a 3.5-mm-thick aluminum plate was attached to both of the detectors. The lifetimes were also measured by another detector configuration to reduce backscattering  $\gamma$  rays between the  $\text{BaF}_2$  detectors. In this configuration, the  $\text{BaF}_2$  detectors were placed at  $90^\circ$  and a 3-mm-thick lead absorber was placed between them. In Sec. III, the former detector configuration will be referred to as the  $180^\circ$  setup, while the latter will be referred to as the  $90^\circ$  setup. The purity of the  $^{68}\text{Cu}^m$  source was monitored through the lifetime measurement by measuring  $\gamma$  rays with a Ge detector.

The  $\text{BaF}_2$  scintillator was mounted on a Hamamatsu-H3378 photomultiplier tube and the time pickoff signals were generated by an ORTEC-583 constant fraction discriminator. An ORTEC-567 time-to-amplitude converter (TAC) was employed and was calibrated using an ORTEC-462 time calibrator. The  $\gamma$ - $\gamma$ - $t$  coincidence data were recorded event by event. An energy resolution was 9% for the 570-keV  $\gamma$  ray of  $^{207}\text{Bi}$ . A typical time resolution of this system was 130 ps at full width at half maximum for the 1173-1332 keV  $\gamma$ -ray cascade of  $^{60}\text{Co}$ .

A  $\gamma$ -ray singles measurement was performed in order to obtain the  $\gamma$ -ray energies and intensities in  $^{68}\text{Cu}$  using an  $n$  type Ge detector of 33% relative efficiency. The distance between the source and the surface of the detector was 102 mm. No  $\beta$ -absorber was placed on this detector. The detection efficiency of the Ge detector was calibrated using a standard source of  $^{152}\text{Eu}$ ,  $^{133}\text{Ba}$ , and  $^{207}\text{Bi}$ , and was corrected for the self-absorption in the  $^{68}\text{Zn}$  target. This absorption was estimated on the basis of the attenuation of the  $\gamma$ -ray intensities measured by putting the standard sources on the  $^{68}\text{Zn}$  target.

### III. RESULTS

Figures 1(a) and 1(b) show  $\gamma$ -ray singles spectra measured with the Ge detector and with the  $\text{BaF}_2$  detector, respectively, in the lifetime measurement. Most of the  $\gamma$  rays observed in the spectra are emitted by  $^{68}\text{Cu}^m$ . Since the ground state of  $^{68}\text{Cu}$  decays to  $^{68}\text{Zn}$  with  $T_{1/2}=31$  s, the  $\gamma$  rays in  $^{68}\text{Zn}$  also appear in these spectra. Although  $\gamma$  rays following the  $\beta$  decay of  $^{67}\text{Cu}$  ( $T_{1/2}=62$  h),  $^{65}\text{Ni}$  ( $T_{1/2}=2.5$  h), and  $^{69}\text{Zn}$  ( $T_{1/2}=14$  h) are also observed, these contributions are small. Figure 1(c) shows a time spectrum measured with the  $\text{BaF}_2$  detectors. It is remarkable that more than half of the coincidence events are due to the decay with a long lifetime for the 84-keV level.

The decay scheme of  $^{68}\text{Cu}^m$  is shown in Fig. 2. Coincidence relationships measured in this work are consistent with the previous scheme [28]. Spin-assignment of the 611-keV level will be discussed in Sec. IV. Figure 3(a) shows a  $\gamma$ -ray spectrum coincident with the 526-keV  $\gamma$ -ray energy (includ-

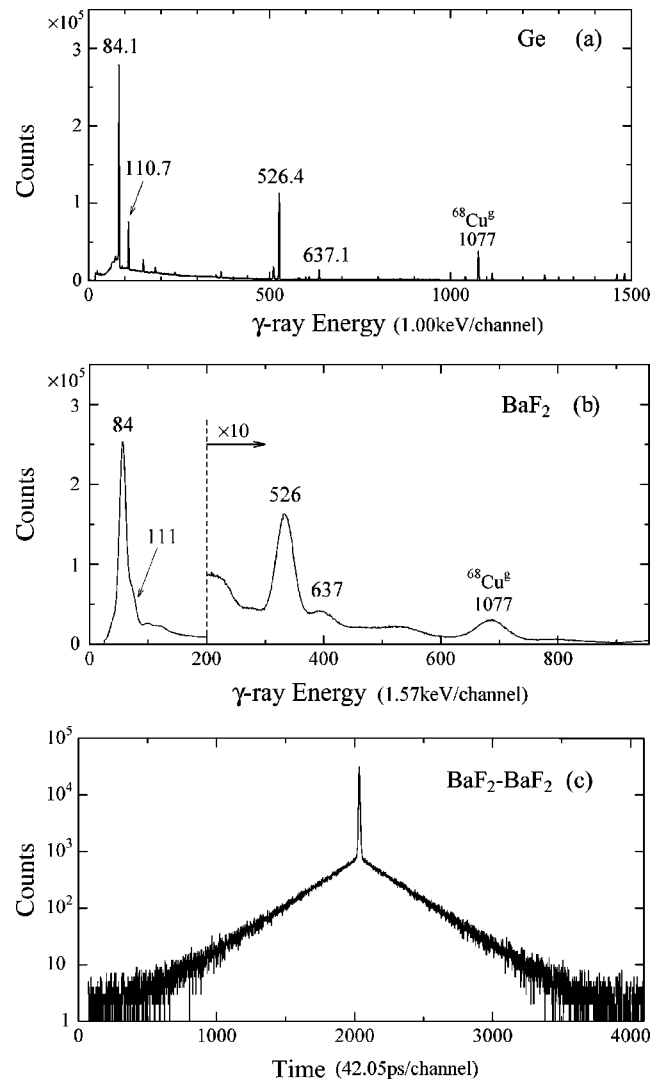


FIG. 1. (a) A  $\gamma$ -ray singles spectrum measured with a Ge detector. The  $\gamma$ -ray energies are depicted for the transitions descending from  $^{68}\text{Cu}^m$ . The 1077-keV  $\gamma$  ray follows the  $\beta$  decay of the ground state in  $^{68}\text{Cu}$ . (b) A  $\gamma$ -ray singles spectrum measured with a  $\text{BaF}_2$  detector. (c) A time spectrum measured by the  $\text{BaF}_2$ - $\text{BaF}_2$ - $t$  coincidence with no gates on  $\gamma$  rays.

ing the Compton continuum under the peak) and with the delayed part, between 4 ns and 87 ns from the prompt peak, of the TAC spectrum. This spectrum was derived from the data of the  $180^\circ$  setup. Figure 3(b) is a  $\gamma$ -ray spectrum coincident with the 526 keV energy and with the prompt part between  $-0.4$  ns and  $+0.4$  ns, derived from the data of the  $90^\circ$  setup. In Fig. 3(a), no other components except for the 84 keV peak are observed. This fact warrants the following lifetime analysis for the 84-keV level.

Decay curves for the 84-keV level were obtained by setting gates on a combination of  $\gamma$ -ray energies measured with the  $\text{BaF}_2$  detectors. Figure 4(a) shows those curves derived from the data of the  $180^\circ$  setup by setting the gates of 526–84 keV and 637–84 keV. The experimental data were fitted with an exponential decay curve,  $a \exp(-\lambda t)$ , by a least squares method and the fitted lines are drawn, as shown in Fig. 4(a), in the range where the experimental data were used

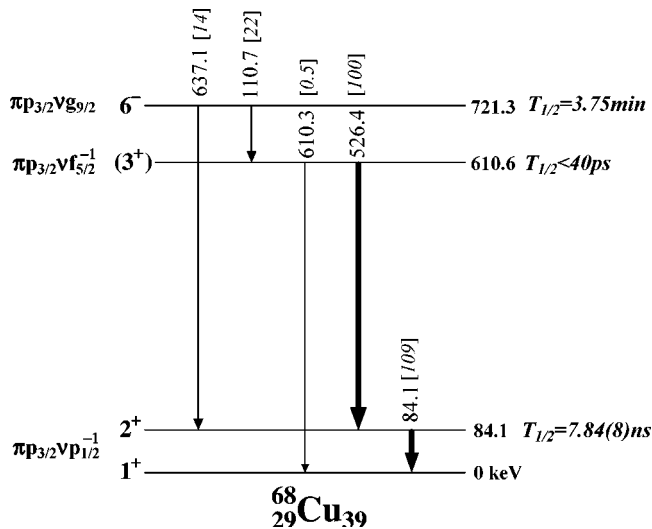


FIG. 2. A decay scheme of  $^{68}\text{Cu}^m$ . The  $\gamma$ -ray and level energies are in units of kilo-electron-volt. Relative intensities are shown in brackets. The lifetime of the  $6^-$  isomer is taken from Ref. [28].

as the input values. We deduced the lifetime of the 84-keV level from the slopes of these fitted lines as well as from those of the decay curves gated on 111–84 keV. All the values of the slopes for the six decay curves are the same within measured uncertainties. Furthermore, the decay curves measured with the  $90^\circ$  setup give the same result. Consequently, we determined that the lifetime of this level is  $T_{1/2}$

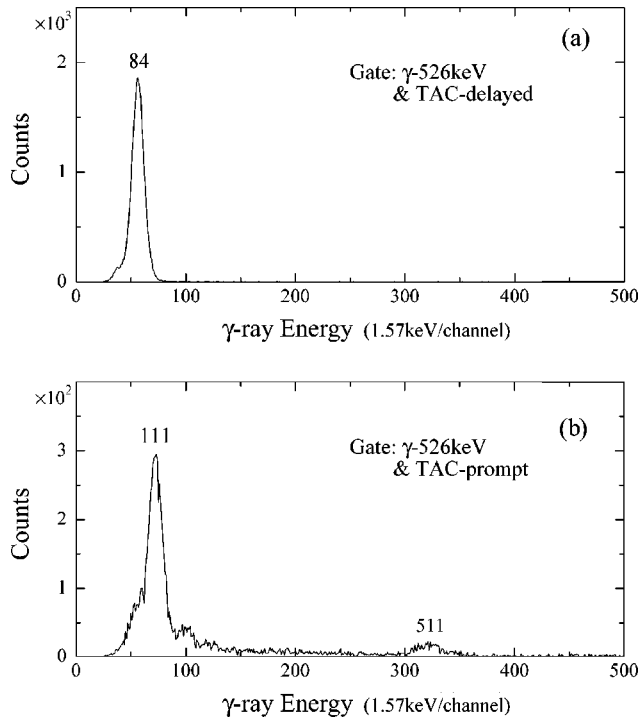


FIG. 3. (a) A  $\gamma$ -ray spectrum in coincidence with the 526-keV  $\gamma$ -ray energy and with the delayed part, between 4 ns and 87 ns from the prompt peak, of the TAC spectrum. (b) A  $\gamma$ -ray spectrum in coincidence with the 526-keV  $\gamma$ -ray energy and with the prompt part between  $-0.4$  ns and  $+0.4$  ns.

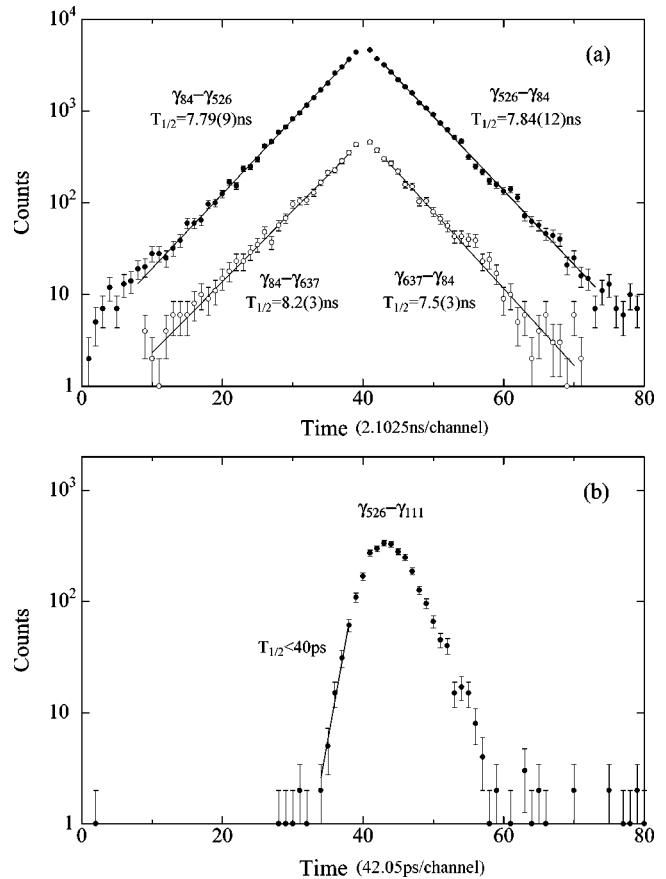


FIG. 4. (a) Decay curves due to the lifetime of the 84-keV level obtained by setting the gates on the  $\gamma$ -ray combinations of 526–84 keV and 637–84 keV. The lines fitted to an exponential decay are drawn in the fitting ranges. (b) A time spectrum for the 611-keV level obtained by the gate on the 526-keV  $\gamma$ -ray energy (start signal) and the 111-keV  $\gamma$ -ray energy (stop signal). The slope of the line drawn in this figure gives an upper limit for the lifetime of the 611-keV level.

$=7.84(8)$  ns. This error was estimated from the spread of all the values obtained in the experiment and from the variation of the values resulting from changing the fitting range. We also ascertained that the contaminant with a long lifetime component is negligible by fitting the experimental data with a curve consisting of an exponential decay and a constant background,  $a \exp(-\lambda t) + b$ .

Figure 4(b) shows a time spectrum obtained by setting the gate on the combination of the 526 keV energy (start signal) and the 111 keV energy (stop signal). This spectrum was derived from the data of the  $90^\circ$  setup. Although this time spectrum includes a component of the Compton continuum under the 111-keV peak as shown in Fig. 3(b), this contribution is only about 10%. Thus, the slope of the line drawn in this figure allows us to deduce an upper limit of 40 ps for the half-life of the 611-keV level.

$\gamma$ -ray energies and intensities in  $^{68}\text{Cu}$  are summarized in Table I. We derived the  $\gamma$ -ray intensities by taking into account the cascade summing effect, although the correction resulting from this effect was about 1% except for the weak 610-keV transition. The intensity of the 610-keV  $\gamma$  ray has a

TABLE I.  $\gamma$ -ray energies and intensities in  $^{68}\text{Cu}$ .

$E_\gamma$ (keV)	$I_\gamma$		$\alpha_T$			
Present work	Present work	Swindle <sup>a</sup>	Tikku <sup>b</sup>	Present work	Swindle <sup>a</sup>	Tikku <sup>b</sup>
84.12(6)	109(4)	96.4(58)	95(5)	0.05(4)	0.156(25)	0.21(7)
110.74(6)	22.2(7)	22.3(13)	24.3(16)	3.52(12)		3.19(22)
526.44(6)	100	100	100			
610.3(3)	0.5(2)	1.4(4)	1.7(5)			
637.14(6)	14.3(4)	11.2(15)	14.7(15)			

<sup>a</sup>Reference [21].

<sup>b</sup>Reference [22].

large error, because it was corrected by considering the sum peak of the 526-keV and the 84-keV  $\gamma$  rays as well as the overlapped 609-keV  $\gamma$  ray following the decay of  $^{214}\text{Bi}$  in the room background. The internal conversion coefficients (ICCs) calculated from the  $\gamma$ -ray intensity balance are also given in Table I. Intensities and ICCs in the previous work [21,22] are shown in this table for comparison.

#### IV. DISCUSSION

We first clarify the difference between the present results and those of previous reports [21,22]. The 611-keV level was previously proposed as  $3^-$  on the basis of the ICC and the lifetime of the 111-keV transition [21,22]. However, the ICC of this transition  $\alpha_T=3.52(12)$  only supports this transition as  $M3$  or  $E3$ ; a theoretical  $\alpha_T$  is 3.71 and 3.75 for an  $M3$  and an  $E3$  transition, respectively [29]. The transition rate of the 111-keV  $\gamma$  ray corresponds to 1.0 W.u. and 0.02 W.u. for  $M3$  and  $E3$ , respectively. There is no reason this transition rate favors an  $M3$  multipolarity. We would rather propose that the spin parity of this level is  $3^+$  on the basis of the following shell model consideration. Low-lying negative-parity states in  $^{68}\text{Cu}$  should have the  $\pi p_{3/2} \nu g_{9/2}$  configuration. All the quartet members of this configuration were clearly observed by the ( $t$ ,  $^3\text{He}$ ) transfer reaction [23]; the  $6^-$  isomer is a member of this quartet and the other members lie above this isomer. Moreover, our recent experiment using heavy-ion deep-inelastic collisions suggests that one of the quartet members at 777 keV has the spin parity of  $3^-$  [25]. On the other hand, the  $3^+$  state with the  $\pi p_{3/2} \nu f_{5/2}^{-1}$  configuration very plausibly exists at 611 keV, because the  $\nu f_{5/2}^{-1}$  state lies at 694 keV in the neighboring nucleus  $^{67}\text{Ni}$  [3].

The intensity of the 84-keV  $\gamma$  ray measured by the present work is also different from the previous ones [19–22]. This intensity affects the estimation of the  $B(M1)$  value of the 84-keV transition, because the  $E2/M1$  mixing ratio of this transition is deduced from the ICC derived from the  $\gamma$ -ray intensity balance. Since all the previous data were measured in the early 1970s, one of the most likely reasons for this discrepancy is that the efficiency calibration of a Ge(Li) detector had a large error in the 80 keV energy region. To obtain a detection efficiency at about 80 keV, one usually uses the standard intensity of the 79.6- and 81.0-keV  $\gamma$  line of the  $^{133}\text{Ba}$  source. This intensity in the references compiled in 1970s [30,31] was smaller than the present one [32] by about

10%. Therefore, the 1970s data of the 84-keV intensity would become smaller than that in the present result.

Now we discuss the  $B(M1; 2^+ \rightarrow 1^+)$  value of the 84-keV transition. From the present result of the ICC of the 84-keV transition,  $\alpha_T=0.05(4)$ , we regard this transition as a pure  $M1$  multipolarity; a theoretical  $\alpha_T$  is 0.086 and 1.18 for a pure  $M1$  and  $E2$  transition, respectively [29]. Then, the  $B(M1)$  value is obtained as  $0.00777(8)\mu_N^2$ , or  $1/230$  W.u., from the measured lifetime of the 84-keV level and the theoretical  $\alpha_T$  for the pure  $M1$  transition.

The  $B(M1)$  value can be estimated by a shell model calculation which takes the core to be  $^{68}\text{Ni}$  and uses experimental  $g$  factors of neighboring nuclei. The  $B(M1)$  value with one proton ( $j_\pi$ ) and one neutron ( $j_\nu$ ) outside the core is calculated as

$$B(M1; I_i \rightarrow I_f) = \frac{3}{4\pi} (2I_f + 1) j_\pi (j_\pi + 1) (2j_\pi + 1) \times W^2(j_\nu j_\pi I_f 1; I_i j_\pi) \times (g_\pi - g_\nu)^2, \quad (1)$$

where  $g_\pi$  and  $g_\nu$  are  $g$  factors of the  $j_\pi$  proton and the  $j_\nu$  neutron, respectively [33]. The  $B(M1)$  value of the 84-keV transition between the  $\pi p_{3/2} \nu p_{1/2}^{-1}$  doublets is

$$B(M1; 2^+ \rightarrow 1^+) = \frac{3}{4\pi} \times \frac{3}{8} \times (g_\pi - g_\nu)^2 = 0.0427 \mu_N^2, \quad (2)$$

where  $g_\pi=1.893\mu_N$  and  $g_\nu=1.202\mu_N$  are taken from the experimental values of the  $3/2^-$  ground state in  $^{69}\text{Cu}_{40}$  and the  $1/2^-$  ground state in  $^{67}\text{Ni}_{39}$ , respectively [13]. This calculation reproduces a small  $B(M1)$  value, which originates from the cancellation of  $g_\pi - g_\nu$ . The  $g$  factor of the  $1^+$  ground state in  $^{68}\text{Cu}$  was also measured recently by a laser-ion-source technique to be  $+2.48(2)(7)\mu_N$  [24]. This  $g$  factor is calculated as

$$g(1^+) = \frac{1}{4} (5g_\pi - g_\nu) = +2.07\mu_N. \quad (3)$$

Thus, the calculation in the  $\pi p_{3/2} \nu p_{1/2}^{-1}$  model space provides a good description of these  $M1$  matrix elements in  $^{68}\text{Cu}$ , using no free parameters. These results are shown in Table II as Cal-A. However, it is difficult to adjust the calculation more accurately for both the  $B(M1)$  value and the  $g$  factor by only changing the  $g_\pi$  and  $g_\nu$  effectively.

TABLE II. Shell model calculations of the  $M1$  matrix elements in  $^{67}\text{Ni}$ ,  $^{69}\text{Cu}$ , and  $^{68}\text{Cu}$ . All the values in the table are in units of  $\mu_N$ . Cal-A,  $\pi p_{3/2} \nu p_{1/2}^{-1}$  model space using the experimental  $g(1/2^-)$  value of  $^{67}\text{Ni}$  and  $g(3/2^-)$  value of  $^{69}\text{Cu}$ . Cal-B1,  $(p_{3/2} f_{5/2} p_{1/2})^n$  model space. Cal-B2,  $f_{7/2}^r (p_{3/2} f_{5/2} p_{1/2})^{n+r}$  ( $r=0, 1$ ) model space. Two-body interactions used in Cal-B1 and Cal-B2 are described in the text.

Nucleus		Cal-A	Cal-B1	Cal-B2	Expt.
$^{67}\text{Ni}_{28}$	$g(1/2^-)$		1.28	0.93	1.20(1) <sup>a</sup>
$^{69}\text{Cu}_{29}$	$g(3/2^-)$		2.53	2.08	1.89(1) <sup>a</sup>
	$g(1^+)$	2.07	2.76	2.60	2.48(2)(7) <sup>b</sup>
$^{68}\text{Cu}_{29}$	$g(2^+)$	1.72	1.89	1.37	
	$\langle 2^+    M1    1^+ \rangle$	0.46	1.04	0.59	0.197(1)

<sup>a</sup>Reference [13].

<sup>b</sup>Reference [24].

This difficulty indicates a limit of this calculation using a minimum model space.

We have further studied the nuclear structure of  $^{68}\text{Cu}$  by a shell model calculation in a  $fp$  model space. To investigate the effect of a  $f_{7/2}$  particle excitation, a shell model calculation of the  $(p_{3/2} f_{5/2} p_{1/2})^n$  model space was compared with that of the  $f_{7/2}^r (p_{3/2} f_{5/2} p_{1/2})^{n+r}$  ( $r=0, 1$ ) model space. In the former calculation Cal-B1, the MSDI two-body interactions by Koops-Glaudemans were used [34]. In the latter calculation Cal-B2, two-body interactions derived from the folded diagram theory were used and single-particle energies were adjusted to reproduce low-lying levels in  $^{67}\text{Ni}$  and  $^{68,69}\text{Cu}$ . The results are summarized in Table II. In Cal-B1, the  $g$  factors of the  $1/2^-$  state in  $^{67}\text{Ni}$  and of the  $3/2^-$  state in  $^{69}\text{Cu}$  correspond to the Schmidt values of the  $\nu p_{1/2}$  and the  $\pi p_{3/2}$  single-particle states, respectively. In Cal-B2, the  $g(3/2^-)$  value of  $^{69}\text{Cu}$  is close to the experiment, while the  $g(1/2^-)$  value of  $^{67}\text{Ni}$  is slightly smaller than the experimental value.

These calculations give a measure of the purity of the  $\pi p_{3/2} \nu p_{1/2}^{-1}$  doublet states in  $^{68}\text{Cu}$ ; the amplitude of the  $\pi p_{3/2} \nu p_{1/2}^{-1}$  component in the  $1^+$  ground state is 0.91 and 0.78

in Cal-B1 and Cal-B2, respectively. The  $g(1^+)$  value of  $^{68}\text{Cu}$  in Cal-B2 is as large as that in Cal-B1. This is in contrast to the Cal-A result giving a smaller value than the experiment. On the other hand, the reduced matrix element of  $\langle 2^+ || M1 || 1^+ \rangle$  in Cal-B2 is much smaller than that in Cal-B1. These calculations show that this matrix element comprises the components originating from protons and from neutrons having a comparable magnitude but an opposite sign and that the difference between these components in Cal-B2 is smaller than that in Cal-B1. Therefore, this  $\langle 2^+ || M1 || 1^+ \rangle$  matrix element has a small value and is sensitive to a  $f_{7/2}$  particle excitation. Although the experimental  $\langle 2^+ || M1 || 1^+ \rangle$  value is still smaller than the Cal-B2 result, the calculation may be improved by extending the model space to include the excitation to a  $g_{9/2}$  orbital.

## V. CONCLUSION

We have measured the lifetime of the first excited state in  $^{68}\text{Cu}$  through the  $\gamma$  decay of  $^{68}\text{Cu}^m$  produced by the  $^{68}\text{Zn}(n, p)$  reaction using 14-MeV neutrons. We obtained a small  $B(M1)$  value between the  $\pi p_{3/2} \nu p_{1/2}^{-1}$  doublet states in  $^{68}\text{Cu}$ . A parameter-free shell model calculation taking the core as  $^{68}\text{Ni}$  gives a good prediction of this  $B(M1)$  value by using experimental  $g$  factors of the  $1/2^-$  state in  $^{67}\text{Ni}$  and the  $3/2^-$  state in  $^{69}\text{Cu}$ . Both the  $B(M1; 2^+ \rightarrow 1^+)$  and the  $g(1^+)$  values in  $^{68}\text{Cu}$  can be explained by a shell model calculation in the  $fp$  model space including a  $f_{7/2}$  particle excitation.

## ACKNOWLEDGMENTS

We would like to acknowledge Dr. T. Nishitani, the group leader of FNS, and the staff of FNS for supporting this experiment. We also thank Dr. A. Taniguchi for important suggestions regarding BaF<sub>2</sub> detectors and also thank Dr. Y. Kasugai for his advice on experiments using fast neutrons. We are grateful to Prof. K. Kawade for his fruitful discussions as well as for kindly allowing us to use the pneumatic tube system. One of us (L.H.) was supported by the MEXT scientist exchange program 2001.

- 
- [1] M. Bernas, Ph. Dessagne, M. Langevin, J. Payet, F. Pougheon, and P. Roussel, Phys. Lett. **113B**, 279 (1982).  
[2] M. Girod, Ph. Dessagne, M. Bernas, M. Langevin, F. Pougheon, and P. Roussel, Phys. Rev. C **37**, 2600 (1988).  
[3] T. Pawlat, R. Broda, W. Królás, A. Maj, M. Ziębliński, H. Grawe, R. Schubart, K. H. Maier, J. Heese, H. Kluge, and M. Schramm, Nucl. Phys. **A574**, 623 (1994).  
[4] R. Broda *et al.*, Phys. Rev. Lett. **74**, 868 (1995).  
[5] R. Grzywacz *et al.*, Phys. Rev. Lett. **81**, 766 (1998).  
[6] S. Franchoo *et al.*, Phys. Rev. Lett. **81**, 3100 (1998).  
[7] T. Ishii, M. Asai, I. Hossain, P. Kleinheinz, M. Ogawa, A. Makishima, S. Ichikawa, M. Itoh, M. Ishii, and J. Blomqvist, Phys. Rev. Lett. **81**, 4100 (1998).  
[8] J. I. Prisciandaro, P. F. Mantica, A. M. Oros-Peusquens, D. W. Anthony, M. Huhta, P. A. Lofy, and R. M. Ronningen, Phys. Rev. C **60**, 054307 (1999).  
[9] W. F. Mueller *et al.*, Phys. Rev. Lett. **83**, 3613 (1999).  
[10] T. Ishii, M. Asai, A. Makishima, I. Hossain, M. Ogawa, J. Hasegawa, M. Matsuda, and S. Ichikawa, Phys. Rev. Lett. **84**, 39 (2000).  
[11] W. F. Mueller *et al.*, Phys. Rev. C **61**, 054308 (2000).  
[12] M. Asai, T. Ishii, A. Makishima, I. Hossain, M. Ogawa, and S. Ichikawa, Phys. Rev. C **62**, 054313 (2000).  
[13] J. Rikowska *et al.*, Phys. Rev. Lett. **85**, 1392 (2000).  
[14] A. M. Oros-Peusquens and P. F. Mantica, Nucl. Phys. **A669**, 81 (2000).  
[15] O. Sorlin *et al.*, Phys. Rev. Lett. **88**, 092501 (2002).  
[16] G. Georgiev *et al.*, J. Phys. G **28**, 2993 (2002).  
[17] H. Grawe *et al.*, Nucl. Phys. **A704**, 211c (2002).  
[18] O. Monnoye, S. Pittel, J. Engel, J. R. Bennett, and P. Van

- Isacker, Phys. Rev. C **65**, 044322 (2002).
- [19] T. E. Ward, H. Ihochi, and J. L. Meason, Phys. Rev. **188**, 1802 (1969).
- [20] H. Singh, V. K. Tikku, B. Sethi, and S. K. Mukherjee, Nucl. Phys. **A174**, 426 (1971).
- [21] D. L. Swindle, N. A. Morcos, T. E. Ward, and J. L. Meason, Nucl. Phys. **A185**, 561 (1972).
- [22] V. K. Tikku and S. K. Mukherjee, J. Phys. G **1**, 446 (1975).
- [23] J. D. Sherman, E. R. Flynn, Ole Hansen, Nelson Stein, and J. W. Sunier, Phys. Lett. **67B**, 275 (1977).
- [24] L. Weissman *et al.*, Phys. Rev. C **65**, 024315 (2002).
- [25] T. Ishii, M. Asai, P. Kleinheinz, M. Matsuda, A. Makishima, T. Kohno, and M. Ogawa, JAERI-Review Report No. 2002-029, 2002, p. 25.
- [26] T. Ishii, M. Itoh, M. Ishii, A. Makishima, M. Ogawa, I. Hossain, T. Hayakawa, and T. Kohno, Nucl. Instrum. Methods Phys. Res. A **395**, 210 (1997).
- [27] K. Kawade, H. Yamamoto, T. Yamada, T. Katoh, T. Iida, and A. Takahashi, JAERI-M Report No. 90-171, 1990.
- [28] R. B. Firestone and V. S. Shirley, *Table of Isotopes*, 8th ed. (Wiley, New York, 1996).
- [29] I. M. Band, M. B. Trzhaskovskaya, and M. A. Listengarten, At. Data Nucl. Data Tables **18**, 433 (1976).
- [30] E. A. Henry, Nucl. Data Sheets **11**, 495 (1974).
- [31] C. M. Lederer and V. S. Shirley, *Table of Isotopes*, 7th ed. (Wiley, New York, 1978), Appendixes-3.
- [32] T. Horiguchi, T. Tachibana, H. Koura, and J. Katakura, *Chart of the Nuclides 2000* (Nuclear Data Center, JAERI, 2000).
- [33] R. D. Lawson, *Theory of the Nuclear Shell Model* (Clarendon, Oxford, 1980), Chap. 5.
- [34] J. Koops and P. M. W. Glaudemans, Z. Phys. A **280**, 181 (1977).